Sensors and Materials, Vol. 15, No. 8 (2003) 393–402
MYU Tokyo

S & M 0537

Improvement of On-Site Microfluidic Benzene, Toluene, Xylene (BTX) Gas Sensor Loaded with Nanostructured Mesoporous Silicate

Yuko Ueno*, Tsutomu Horiuchi, Osamu Niwa, Hao-shen Zhou[1], Takeo Yamada[1] and Itaru Honma[1]

NTT Microsystem Integration Laboratories
3-1 Morinosato Wakamiya, Atsugi, Kanagawa 243-0198, Japan
[1]National Institute of Advanced Industrial Science and Technology

(Received September 1, 2003; accepted October 28, 2003)

Key words: BTX gas, mesoporous silicate, microfluidic device

We have developed a gas sensing microfluidic device for the detection and identification of aromatic volatile organic compound (VOC) gases, namely, benzene, toluene, and xylenes (BTX), which are air pollutants. We combined a nanostructured material, mesoporous silicate, as a gas concentrator and separator, and carried out spectroscopic measurement with a microfluidic device for gas identification and quantitative detection. Our method is completely different from conventional methods such as gas chromatography (GC)/mass spectrometry(MS) and provides a portable, highly sensitive and selective gas monitoring system. In this paper, we report an improvement in the performance of our BTX gas sensor that we realized by optimizing the operating conditions and by using the properties of mesoporous silicate with uniform nanosized pores. We also successfully measured mixture BTX gases separately with this device. We were able to realise better BTX separation with mesoporous silicate than with random-structured silicates. We successfully analyzed the principle behind the improvement in the gas separation owing to the characteristics of the nanosized pores of mesoporous silicate by positron annihilation spectroscopy.

*Corresponding author, e-mail address: ueno@aecl.ntt.co.jp

1. Introduction

Airborne benzene, toluene, and xylenes (BTX) are volatile organic compounds (VOCs) of significant concern as regards environmental health due to their toxicity and mutagenetic or carcinogenetic properties, even at ppb concentrations. In particular, benzene is a well-known human carcinogen for all routes of exposure and is a risk factor for leukemia and lymphomas.[1] The fact that these VOCs have very different toxicities has meant that society has dealt with them differently. The regulated standard concentrations of benzene are 1, 3 and 5 $\mu g/m^3$ (0.33, 1.0 and 1.6 ppb) in the United States,[2] Japan[3] and the European Union,[4] respectively. The guideline values for indoor upper concentration limits of toluene and xylenes in Japan are 260 and 870 $\mu g/m^3$ (0.07 and 0.20 ppm), respectively. Since BTX gases are the main components of automobile exhaust, this is the primary source of benzene emissions (more than 80%). It is obvious that their concentration in the air depends on time and location. This makes it important to determine the concentration of each compound in the air separately for multipoint on-site field monitoring. A portable system is therefore required for on-site monitoring that can detect each BTX species. The most widely used conventional method for VOC detection is GC/MS. The TO-14 method developed by the United States' Environmental Protection Agency (EPA) employs this approach[5] because it has several advantages, namely a ppt detection limit, high selectivity, and high accuracy. However, in terms of field monitoring, it has a crucial disadvantage in that the size and weight of the GC/MS instrument can only be reduced to a certain extent without degrading its selectivity and sensitivity. In contrast, there are several miniature devices for VOC detection including a photo ionization detector and a surface acoustic wave detector, but they have a limited ability to identify individual compounds. Thus, we have developed a portable BTX gas sensor by incorporating two 1 cm × 3 cm microfluidic devices with peripheral devices.[6] This is because microfluidic devices, which are used as platforms for various types of chip-based chemical analysis and have received significant attention over the past decade, have a number of merits when employed as airborne BTX sensors. These advantages include accurate fluid manipulation, a higher throughput, shorter analysis times, reduced sample volumes, the potential for *in situ* operation and reduced manufacturing and operating costs.

We then thought that the combination of the microfluidic device and nanostructured materials would enable us to realize an ideal sensor because it would allow us to fabricate any required sensor by using tailor-made materials without any great change in the device platform. In general, if we wish to provide the sensor system with functions involving molecular interaction levels, we require either a nanoscale fabrication method or a self-assembly processing technique. However, fabricating a device with a specific and complicated structure using advanced micro-fabrication techniques may be very expensive and time consuming and inconvenient as regards minor improvements to the device. From this standpoint, nanosized materials with controllable structures may be the key to obtaining the desired devices. One notable class of nanostructured materials consists of tailored porous materials, and great progress has been made with these over the past decade. Since molecules adsorbed in nanosized pores can behave differently from those adsorbed on a 2D surface, we can use this particular property to develop new adsorbents and catalysts.

Mesoporous silicate is one of a number of typical ordered nanosized structure materials that have attracted considerable interest because of their great potential for a wide range of applications including catalysis,[7] catalytic supporters,[8] molecular sieves,[9] adsorbents[10] and nanotechnology.[11] Zhao *et al.* synthesized novel ordered mesoporous silicates using a commercially obtained triblock copolymer, star diblock copolymer and oligomeric surfactants as a template agent to obtain several different porous structures.[12] When preparing periodic porous structured materials with larger pores (2 to 50 nm), triblock templating is better than using zeolites or ionic-surfactant-templated mesoporous silicates such as MCM-41, as regards incorporating molecules or functional groups into pores.

We employed mesoporous silicate powder (SBA-15) as an adsorbent for our BTX gas sensor. The most important properties are pore structure and pore size controllability, which we achieved using a specified template agent and synthesis conditions. In our previous study, we achieved a 10 ppb detection limit for toluene with a sampling time of 30 min.[13] We also succeeded in the separate detection of the components of 10 ppm of BTX mixture gas using the characteristics of mesoporous silicate with uniform nanosized pores. This was due to an enhancement of the differences between the thermal desorption properties of benzene, toluene, and *o*-xylene caused by the repetition of the adsorption-desorption process in a nanosized column.[14]

In this paper, we report an improvement in our BTX gas sensor performance that we achieved by optimizing the operating conditions and using the characteristics of mesoporous silicate with uniform nanosized pores.

2. Materials and Methods

Figure 1 shows a schematic view of our microfluidic device with peripheral devices. The concentration and detection cells both consist of two Pyrex plates each 3 cm × 1 cm in size. For the concentration cell, we fabricated a microchannel, and inlet and outlet holes, and formed a thin-layer heater outside the channel. There is a shallow section in the middle of the channel to prevent the packed adsorbent from moving. The adsorbent we used was commercially obtained amorphous silicon dioxide powder (SDP) and mesoporous silicate powder (SBA-15). Of the ordered mesoporous silicate family, hexagonally ordered SBA-15, which was synthesized using a triblock copolymer EO_{20}-PO_{70}-EO_{20} (BASF Corporation: Pluronic P123; M_w = 5750) as a template agent, is currently the most widely used due to its stability with respect to the synthesis conditions. We therefore employed SBA-15, which we synthesized using a method described elsewhere.[12] We packed the concentration cell channel (width = 2.5 mm, depth = 0.2 mm, length = 7 mm of packing area) with ~0.5 mg of SBA-15 that corresponds to ~5 mm length in the channel. For the detection cell, we also fabricated a microchannel, and inlet and outlet holes. Both ends of the channel were sealed with optical fibers and the channel was aligned between a UV light source (30 W deuterium (D_2) lamp, Soma Optics) and a UV spectrometer (specially modified Fastevert S-2400, Soma Optics). We have detailed the structures of the concentration and detection cells and the fabrication process elsewhere.[6] We installed the concentration and detection cells, the UV light source, the UV spectrometer, a palm-size piezoelectric pump (Bimor pump, Kyokko Co., Ltd., BPF-465P, 7.2 cm × 7.2 cm × 3.2 cm), an SCSI interface and a

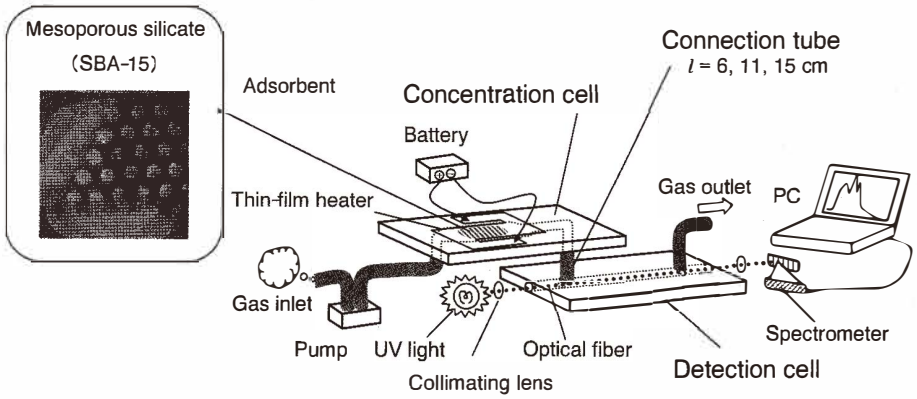

Fig. 1. Schematic view and photograph of microfluidic device with peripheral devices.

controller in our portable BTX automatic gas measurement system (38 cm × 28 cm × 12 cm). The measurement procedure is performed automatically once the start button has been pushed. First, a BTX mixture gas is sampled for a certain time. The background spectrum is measured while the gas is being sampled. Then the temperature is raised using a thin-film heater so that the concentrated BTX mixture gas is thermally desorbed from the adsorbent in accordance with the desorption temperatures of benzene, toluene and *o*-xylene. We then introduce desorbed gas into the detection cell along with a carrier gas, namely the original BTX mixture gas we used as a sample. The time-dependent absorption spectra of the desorbed gas are measured in the detection cell. All adsorbate components are removed from the adsorbent by keeping it at 200°C for a few minutes while the gas is flowing. Lastly, all the devices are turned off and they remain in the standby mode for the next measurement. The on-off timing of the pump, the heater and the spectrometer are precisely controlled by a PC to obtain the optimum performance.

To provide an artificial environment of BTX-polluted air, we prepared benzene and toluene gases by diluting commercial-grade benzene (50 ppm) and toluene (50 ppm) gases with nitrogen in a gas blender consisting of mass-flow meters (Estec, SEC-400). We were able to vary the gas flow rate by changing the output frequency of the pump. Here, we set the output frequency at 100 Hz, which gave us a flow rate of approximately 1.1×10^{-1} cm^3 / s at the point furthest downstream from the device.

We were able to detect and identify BTX gases by observing the specific peaks of each compound in the absorption spectra. Since we measured only the 235.0 – 274.5 nm region, the absorption peaks of other gases, for example, water, aliphatic compounds, and polycyclic aromatic hydrocarbons, do not interfere with the specific peaks of the BTX gases. Here, we used the absorbances of the peaks at 252 and 267 nm for the signal intensities of the detected benzene and toluene gases (S_b and S_t), respectively.

3. Results and Discussion

3.1 *Improvement by optimizing the operating conditions*

3.1.1 *Gas sampling time and signal intensity*

It is very important to study to what extent gases can be concentrated in the adsorbent against time to achieve a low detection limit for each gas. Therefore, we studied the gas sampling time (T_s) dependences of S_b and S_t for 2.5 ppm of benzene gas and toluene gas (Fig. 2). We found that S_b had a larger value than S_t, particularly in the shorter T_s region. This indicates that, at room temperature (approximately 25°C), benzene has a greater affinity to the surface of SBA-15 than to that of toluene. S_b and S_t were not proportional to T_s and increased towards certain saturation levels, and S_b reached the plateau in a shorter T_s than S_t. We believe that one of the main reasons for the signal saturation was that the adsorbed gases broke through from the adsorbent. Since we packed only 5 mm of adsorbent in the channel, it is difficult to avoid the gases breaking through with a long T_s.

For a gas sensor, a shorter T_s is preferable as long as we can obtain a sufficiently large signal. We found that T_s = 5 min is sufficient to obtain S_b or S_t with a signal-to-noise ratio (S/N) of greater than 3 in this concentration region.

3.1.2 *Spectral accumulation time and signal-to-noise ratio*

Next, in order to obtain the optimize S/N, we studied the spectral measurement condition, namely, the total accumulation time required to measure each spectrum (t_e). We

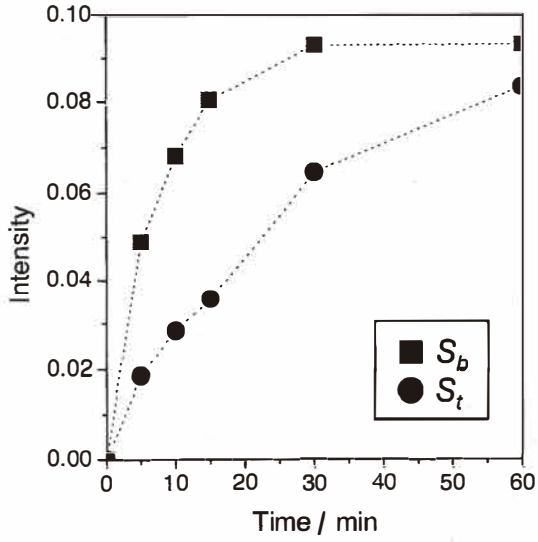

Fig. 2. T_s dependence of S_b (■) and S_t (●). The concentration was 2.5 ppm for both benzene and toluene gases.

measured the S/N at t_e = 0.1, 0.2 and 0.5 s for benzene and at 1.0, 2.0 and 5.0 s for toluene by varying the time the detector was exposed to UV light. We sampled 2.5 ppm each of benzene and toluene gas for 5 min at the flow rate described above (1.1×10^{-1} cm^3 / s). Table 1 shows the t_e dependence of S_b, S_t, the noise level and the S/N ratio. The noise levels were obtained from the standard deviations of the blank spectra in the 235.0 – 274.5 nm region. We found that S_b and S_t decreased with increasing t_e due to the leveling off of the peak. In contrast, the noise level decreased and was almost inversely proportional to the square root of t_e. We found that the t_e values that gave the largest S/N were 0.2 and 2.0 s for benzene and toluene detection, respectively. The reason for the almost tenfold difference between the t_e values for benzene and toluene can be attributed to the different bandwidths of S_b and S_t.

3.2 *Improvement using mesoporous silicate*

Figure 3 compares changes in the signal intensities of benzene, toluene, and *o*-xylene with time when using SBA-15 (a) and SDP (b) that were measured using the same settings that we used in the previous sections. We set the time at which we turned the pump on at zero seconds, 7.0 s after the thin-film heater was turned on (the thin-film heater reaches a higher temperature than the boiling point of *o*-xylene 7.0 s after being turned on). The order in which the compounds were detected was the same for both SBA-15 and SDP, namely benzene, toluene, and then *o*-xylene. The response time and the signal intensities were different from those of the previous study because we have improved such operating conditions as the temperature elevation rate, the gas flow rate, the power of the light introduced into the detection cell, and the arrangement of the microdevice in relation to the peripheral devices. We observed that SBA-15 provided sharper peaks while SDP provided broader peaks, in spite of the small differences between the adsorption energies of benzene, toluene, and *o*-xylene on both the silicate surfaces. This indicates that SBA-15 provides response curves with much better separation than does SDP. Table 2 shows the times at which the benzene, toluene, and *o*-xylene signals reached their median values. The separation of benzene - toluene and that of toluene-*o*-xylene were improved by 0.2 to 0.6 s (300%) and 0.2 to 0.8 s (400%), respectively.

Table 1
t_e dependence of S_b and S_t, noise levels and S/N.

Benzene

t_e / s	S_b	noise	S / N
0.1	0.0468	0.0100	4.7
0,2	0.0415	0.0060	6.9
0,5	0.0200	0.0036	5.6

Toluene

t_e / s	S_t	noise	S / N
1.0	0.0148	0.0032	4.6
2.0	0.0129	0.0020	6.5
5.0	0.006	0.0012	5.2

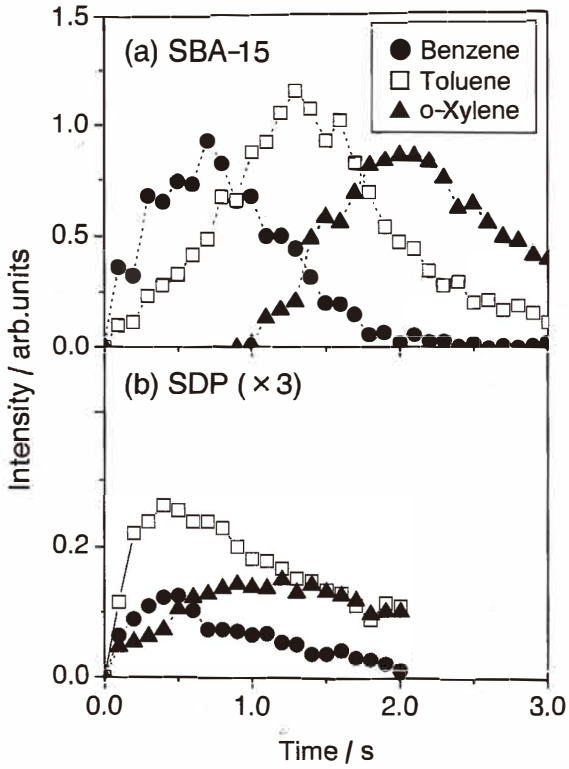

Fig. 3. Changes in signal intensities against time when SBA-15 and SDP are used. We accumulated 50 sets of 10-ms exposure data. Thus, the total time required to measure each spectrum was 0.5 s. To study the changes in shorter time steps, we repeated the measurement, on this occasion delaying the measurement starting time by 0.1 s, and overlaid the results.

Table 2
Times at which the benzene, toluene and *o*-xylene signals reach their median values.

	Benzene	Toluene	*o*-Xylene
	Time at median / s		
SBA-15	0.7	1.3	2.1
SDP	0.6	0.8	1.0

We then investigated the main mechanism involved in the improved separation of SBA-15. If the main mechanism is explained by the uniform mesopore structure, the interaction between the adsorbate gases and the surface should be stronger with SDP than with SBA-15. This is because the mesopores of SBA-15 are much larger than those of

SDP. However, the benzene, toluene, and *o*-xylene signals took longer to reach their mean values with SBA-15 than with SDP. This shows that the interaction between the adsorbate gases and the surface is stronger with SBA-15 than with SDP, that is, the main reason for the improved separation is not the mesopore structure. Moreover, both the signal intensities (peak areas /peak heights) of benzene, toluene, and *o*-xylene and the ratio of the signal intensity of benzene to that of toluene/*o*-xylene, were larger with SBA-15 than with SDP. This also indicates that the micropore structure affects not only the separation profiles but also the interaction between the adsorbate gases and the pore surface.

Then, in order to analyze the mechanisms that cause the difference between the desorption profiles, we studied the micropore structures of SDP and SBA-15 in detail by using positron annihilation spectroscopy[15] and the nitrogen isotherm. Positron annihilation spectroscopy is not as widely used for micropore analysis as t-curve analysis of the nitrogen isotherm,[16] however, the former technique offers certain benefits. Positron annihilation spectroscopy does not require standard nitrogen adsorption data to obtain the pore distribution. Moreover, it enables us to obtain the pore size distribution in 0.01-nm steps. Figure 4 shows the micropore radius (r_p) distribution of SDP and SBA-15. The full-width at half maximum of SBA-15 was smaller than 0.1 nm indicating that the micropores have a very sharp distribution (a Si-O bond is approximately 0.16 nm), whereas the SDP distribution had two peaks and was widely spread. It is impossible to analyze a pore size distribution that has multipeaks by t-curve analysis. However, we were able to observe that the shape of the "knee" of the t-curves was looser with SDP than with SBA-15, which indicates that the micropore size distribution of the SDP is much broader than that of SBA-15. The results we obtained by t-curve analysis corresponded well with the results we obtained by positron annihilation spectroscopy. The average SBA-15 pore diameter ($2t$, $2r_p$) was 0.7 nm with both approaches (Table 3). Thus we conclude that a uniform pore size

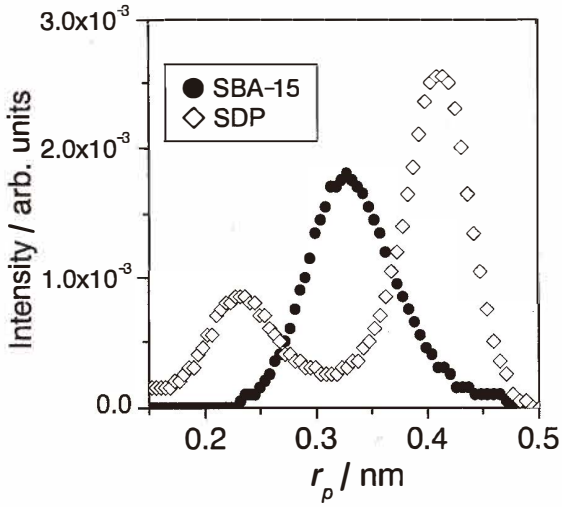

Fig. 4. Micropore radius (r_p) distributions of SDP (◇) and SBA-15 (●) calculated using the positron annihilation spectrum.

Table 3
Porous parameters of SBA-15 and SDP calculated [a]by the Brunauer-Emmett-Teller(BET) method, [b]from *t*-curves and [c]from positron annihilation spectra.

	Surface area S_{BET}[m^2/g][a]	Micropore diameter 2t[nm][b]	Micropore diameter $2r_p$[nm][c]	Pore volune V[nm^3][c]
SBA15	758.39±13.16	0.7±0.1	0.696	0.176
SDP	290.65±4.8	-	-	0.220

of approximately 0.7 nm enables the uniform thermal desorption of BTX gases, and this means we can obtain better BTX separation than with SDP.

4. Conclusion

We optimized several operating conditions of our BTX gas sensor in order to obtain the optimal S_b and S_t responses. We found that a sampling time $T_s = 5$ min is sufficient to obtain S_b or S_t with an S/N ratio of greater than 3 with 2.5 ppm of benzene or toluene gas, and the exposure times, t_e, that gave the largest S/N ratio were 0.2 and 2.0 s for benzene and toluene detection, respectively. We also found that the uniform micropore structure of SBA-15 allows the uniform thermal desorption of BTX gases and this means we can obtain better BTX separation than with SDP. We used positron annihilation spectroscopy to show that the uniformity of the SBA-15 micropores is greater than that of SDP.

References

1 See, for example: Carcinogenic Effects of Benzene: An Update, 1998; EPA/60/P-97/001F; U. S. Environmental Protection Agency, U.S. Government Printing Office: Washington, DC, 1998.
2 National Air Toxics Program: The Integrated Urban Strategy, Report to Congress, 2000; EPA-453/R-99-007; U. S. Environmental Protection Agency, U.S. Government Printing Office: Washington, DC, 2000.
3 Environmental Quality Standards in Japan-Air Quality-, Environmental Quality Standards of Benzene, Trichloroethylene and Tetrachloroethylene, 1997; http://www.env.go.jp/en/lar/regulation/aq.html; Ministry of the Environment, Government of Japan.
4 Are we moving in the right direction? TERM 2000. Environmental issues series No 12, 2000; http://reports.eea.eu.int/ENVISSUENo1 2/en/page008.html; European Environment Agency.
5 Compendium of Methods for the Determination of Toxic Organic Compounds in Ambient Air, 2nd ed.; 1999; EPA/625/R-96/010b; Method TO-14A.
6 Y. Ueno, T. Horiuchi, T. Morimoto and O. Niwa: Anal. Chem. **73** (2001) 4688.
7 C. W. Jones, K. Tsuji and M. E. Davis: Nature **393** (1998) 393.
8 V. S-Y. Lin, D. R. Radu, M-K. Han, W. Deng, S. Kuroki, B. H. Shanks and M. Pruski: J. Am. Chem. Soc. **124** (2002) 9040.
9 E. Prouzet, F. Cot, G. Nabias, A. Larbot, P. Kooyman and T. J. Pinnavaia: Chem. Mater. **11** (1999) 1498.

10 H. Suda and K. Haraya: J. Phys. Chem. B **101** (1997) 3988.
11 P. Yang, G. Wirnsberger, H. C. Huang, S. R. Cordero, M. D. McGehee, B. Scott, T. Deng, G. M. Whitesides, B. F. Chmelka, S. K. Buratto and G. D. Stucky: Science **287** (2000) 465.
12 D. Zhao, Q. Huo, J. Feng, B. F. Chmelka and G. D. Stucky: J. Am. Chem. Soc. **120** (1998) 6024.
13 Y. Ueno, T. Horiuchi and O. Niwa: Anal. Chem. **74** (2002) 1712.
14 Y. Ueno, T. Horiuchi, M. Tomita, O. Niwa, H-S. Zhou, T. Yamada and I. Honma: Anal. Chem. **74** (2002) 5257.
15 P. Hautojarvi, ed.: Positrons in Solids (Springer, Berlin ,1979).
16 B. C. Lippens and J. H. de Boer: Catalysis **4** (1965) 319.